# Experimental test of state-independent quantum contextuality of an indivisible quantum system

Yun-Feng Huang, Meng Li, Dong-Yang Cao, Chao Zhang, Yong-Sheng Zhang, Bi-Heng Liu, Chuan-Feng Li, and Guang-Can Guo

Phys. Rev. A **87**, 052133 — Published 24 May 2013

DOI: 10.1103/PhysRevA.87.052133

# Experimental test of state-independent quantum contextuality of an indivisible quantum system

Yun-Feng Huang,[1,*] Meng Li,[1] Dong-Yang Cao,[1] Chao Zhang,[1] Yong-Sheng Zhang,[1] Bi-Heng Liu,[1] Chuan-Feng Li,[1,†] and Guang-Can Guo[1]

[1]*Key Laboratory of Quantum Information, University of Science and Technology of China, CAS, Hefei, 230026, China*

we report a state-independent experimental test of quantum contextuality of a single-photon qutrit. The experiment results demonstrate violations of an inequality originally formulated by Yu and Oh [Phys. Rev. Lett. **108**, 030402 (2012)] and further optimized by Cabello et al. [Phys. Rev. A **85**, 032108 (2012)]; this inequality is satisfied by all non-contextual hidden variable models and is violated by all qutrit states. Our experiment shows quantum contextuality of the nature in a most fundamental way: a way that is independent of state and unrelated to entanglement.

PACS numbers:

## I. INTRODUCTION

One important attribute of quantum mechanics is that it does not allow observables to have definite values until they are measured. This unusual feature has led to a long-lasting debate on the completeness of quantum mechanics[1]. Thus, hidden variable models, in which all observables do have definite values determined by some hidden variables, cannot be introduced. For a classical model, noncontextuality is believed to be a typical property: the measurement result for an observable is independent of which other compatible observables are measured simultaneously. Local variable models are noncontextual hidden variable (NCHV) models, but in general, NCHV models do not require any further assumptions, such as spacelike separation, on the compatible observables being simultaneously measured. Thus NCHV models more directly reveal the basic idea of hidden variable theories.

In the 1960's, it was proven[2, 3] that NCHV models are not compatible with quantum mechanics (QM). After that, some experimental tests on quantum contexuality were carried out[4–8], employing two qubits and depending on special quantum states. More recently, a state-independent experimental test using two qubits was proposed[9] and performed with trapped ions[10]. In 2011, a state-dependent experimental test using a three-level system (a qutrit), which is the simplest system for testing quantum contextuality, was accomplished[11].

The original theorem in [2] contains a rather complex formulation, and hence, various simplified proofs of quantum contextuality have subsequently been presented[14–16]. For quantum contextuality, there are two important features: the first is that it can be shown even in simple indivisible quantum systems, such as a qutrit[17]. The other feature is that quantum contextuality does not depend on the special form of the quantum state. However, proofs containing both of these features, i.e. the state-independent Kochen-Specker (KS) proofs for a qutrit, are complicated and involve

*Electronic address: hyf@ustc.edu.cn
†Electronic address: cfli@ustc.edu.cn

too many observables to be measured[18–20]. In 2012, Yu and Oh[12] derive a greatly simplified state-independent KS inequality for qutrits, which involves only 13 observables and, at most two compatible observables that must be measured simultaneously. Yu and Oh's inequality is then optimized for larger violations[13], so that an experimental test is more feasible. In this study, we report an experimental test of state-independent quantum contextuality of a single-photon qutrit. Our results show obvious violations of the inequality in [13].

## II. THEORETICAL SCHEME

Consider a qutrit and a set of 13 two-outcome observables[12] $A = \{A_i \mid i = 1, 2, ..., 13\}$, where $A_i == I - 2\left|a_i\right\rangle\left\langle a_i\right|$, in which $I$ is a $3 \times 3$ identity matrix and $\{\left|a_i\right\rangle\}$ are the following three-dimensional unit vectors:

$$\begin{aligned} a_1 &= \frac{1}{\sqrt{3}}(-1,1,1) \qquad a_{7,8} = \frac{1}{\sqrt{2}}(1,0,\pm 1) \\ a_2 &= \frac{1}{\sqrt{3}}(1,-1,1) \qquad a_{9,10} = \frac{1}{\sqrt{2}}(1,\pm 1,0) \\ a_3 &= \frac{1}{\sqrt{3}}(1,1,-1) \qquad a_{11} = (1,0,0) \\ a_4 &= \frac{1}{\sqrt{3}}(1,1,1) \qquad a_{12} = (0,1,0) \\ a_{5,6} &= \frac{1}{\sqrt{2}}(0,1,\pm 1) \quad a_{13} = (0,0,1). \end{aligned} \tag{1}$$

Measurement of $A_i$ gives a result of $+1$ or $-1$. The compatibility (orthogonality) relationships among the 13 observables can be described by a $13 \times 13$ symmetric matrix $\Gamma$ with vanishing diagonal elements. The matrix element $\Gamma_{i,j}$ has only two possible values 0 and 1. If $\Gamma_{i,j} = 1$, $A_i$ and $A_j$ are compatible observables; otherwise, $A_i$ and $A_j$ are not compatible. All 24 nonzero $\Gamma_{i,j}$ $(i < j)$ are listed below:

$$\begin{gathered} \Gamma_{1,6} = \Gamma_{1,7} = \Gamma_{1,9} = 1; \\ \Gamma_{2,5} = \Gamma_{2,8} = \Gamma_{2,9} = 1; \\ \Gamma_{3,5} = \Gamma_{3,7} = \Gamma_{3,10} = 1; \\ \Gamma_{4,6} = \Gamma_{4,8} = \Gamma_{4,10} = 1; \\ \Gamma_{5,6} = \Gamma_{5,11} = 1;\ \Gamma_{6,11} = 1; \\ \Gamma_{7,8} = \Gamma_{7,12} = 1;\ \Gamma_{8,12} = 1; \\ \Gamma_{9,10} = \Gamma_{9,13} = 1; \Gamma_{10,13} = 1; \\ \Gamma_{11,12} = \Gamma_{11,13} = 1; \Gamma_{12,13} = 1. \end{gathered} \tag{2}$$

By denoting the mean value of measurement $A_i$'s outcomes by $\langle A_i \rangle_C$ and denoting the mean value of the product of $A_i$ and $A_j$ measurement outcomes by $\langle A_i A_j \rangle_C$ in NCHV models, Yu and Oh obtain the following inequality

$$S_C = \sum_{i=1}^{13} \langle A_i \rangle_C - \frac{1}{4} \sum_{i,j=1}^{13} \Gamma_{i,j} \langle A_i A_j \rangle_C \leq 8, \tag{3}$$

which all NCHV models should obey. However, for the left-hand side of the inequality in Eq. (3), QM predicts that

$$S_{QM} = \sum_{i=1}^{13} \left\langle \hat{A}_i \right\rangle - \frac{1}{4} \sum_{i,j=1}^{13} \Gamma_{i,j} \left\langle \hat{A}_i \hat{A}_j \right\rangle = \frac{25}{3} \tag{4}$$

for any qutrit state. Thus, a state-independent conflict between QM and NCHV models for single qutrits is obtained.

In [13], it is proven that this inequality can be further optimized by only changing some coefficients. The new inequality reads

$$\begin{aligned} S'_C = \frac{1}{2}(\sum_{i=1}^{4} \langle A_i \rangle_C - \sum_{i=1}^{4}\sum_{j=5}^{10} \Gamma_{i,j} \langle A_i A_j \rangle_C) \\ +\sum_{k=5}^{13} \langle A_k \rangle_C - \sum_{m=5}^{12} \sum_{n>m}^{13} \Gamma_{m,n} \langle A_m A_n \rangle_C \leq 9, \end{aligned} \tag{5}$$

while for quantum mechanics,

$$S'_{QM} = \frac{29}{3}. \tag{6}$$

The new inequality leads to a greater contrast between NCHV and QM predictions, hence, making an experimental test easier and more convincing. Thus, we chose to test inequality Eq. (5).

For an experimental test of noncontextuality, two important requirements need to be considered[13]: One is that the measurement device for each observable $A_i$ should be physically identical in every experimental context. The other is that the setup should permit all possible combinations of measurement results, including outcomes that should never emerge in QM's predictions of an ideal experiment. To satisfy these requirements, we use sequential measurements to measure $A_i A_j$ and adopt the idea of a cascade setup from [13]: (i) For each single observable, a fixed single-observable measuring device is constructed as the basic building block of the experiment. (ii) The input state is first sent to the measurement device of $A_i$, and then the two output parts, corresponding to $A_i = +1$ and $A_i = -1$, are each connected to an identically constructed device to measure $A_j$.

## III. EXPERIMENT SETUP AND RESULTS

In our experiment, we use heralded single photons generated from a spontaneous parametric down-conversion (SPDC) process. By employing the polarization and path degrees of freedom of a single photon, we can prepare arbitrary states of a qutrit. Beam displacers (BDs), which transmit vertically polarized photons while displacing horizontally polarized photons, and half-wave plates (HWPs) are used to manipulate these two degrees of freedom. Thus, the system always consists of one photon with two paths. In one path (the upper path), the photon can be a superposition of a horizontal component ($|H\rangle$) called state $|1\rangle$ and a vertical component ($|V\rangle$) called state $|2\rangle$. In the other path (the lower path), the photon is always polarized horizontally at some places and vertically at other places. When the photon is in this latter path, it is said to be in state $|0\rangle$. Thus, these states: $|0\rangle$, $|1\rangle$ and $|2\rangle$ form the

qutrit's basis. The transformations among them can be simply realized using only a few HWPs and BDs. Figure 1 shows the single-observable measurement setups for $A_3$, $A_7$ and $A_{11}$, which are typical examples among the 13 single observables.

Our experimental setup is illustrated in Figure 2. Photon pairs are generated from the SPDC process in a $\beta$-barium borate (BBO) crystal. One photon is directly detected by $D_0$ as a trigger. The other photon is prepared in the desired qutrit state. To illustrate the state-independence of our test, we prepared the 8 different qutrit states listed in Table 1, including a maximally mixed state $\rho_I$. The first 7 pure states are prepared by a polarizer (P), $HWP1$, $BD1$, $HWP2$ and $HWP3$ in the state preparation stage of Figure 2. To prepare $\rho_I = \frac{1}{3}(|0\rangle\langle 0| + |1\rangle\langle 1| + |2\rangle\langle 2|) = \frac{1}{3}I$, $HWP1$, $HWP2$ and $HWP3$ are set to prepare the photon in the pure state $\frac{1}{\sqrt{3}}(|0\rangle + |1\rangle + |2\rangle)$, and then two birefringent crystals (1.2- $mm$-thick $YVO_4$ crystals, not shown in Figure 2) are inserted after $HWP1$ and $HWP2$. Each birefringent crystal introduces a large enough time delay between $|H\rangle$ and $|V\rangle$ components when the photons pass through it, so that the two birefringent crystals can completely destroy the coherence among $|0\rangle$, $|1\rangle$ and $|2\rangle$ components of the pure state $\frac{1}{\sqrt{3}}(|0\rangle + |1\rangle + |2\rangle)$. Thus, the maximally mixed state $\rho_I$ is produced.

To measure the two compatible observables $\langle A_i A_j\rangle$, the setup in Figure 2 is divided into four parts. Part I is the state preparation stage. In part II, $A_i$ is measured with three HWPs and one BD. The angle settings of $HWP4$, $HWP5$ and $HWP7$ are chosen to project the eigenstate corresponding to $A_i = -1$ onto the $|H\rangle$ mode after $HWP7$, while the other eigenstates with $A_i = +1$ are projected onto the upper path after $BD2$ or the $|V\rangle$ mode after $HWP7$. Then, in part III, $A_j$ is measured. Two identical $A_j$ measuring devices are built, and each is connected to the corresponding output port of the measuring device of $A_i$. Note that before connecting one output port of the $A_i$ measuring device, we need to re-create the corresponding eigenstate of $A_i$, as our single-observable measuring devices map its eigenstates to a fixed spatial path and polarization[21]. As shown in Figure 2, this is achieved with the BDs and HWPs between part II and III: First we separate the $A_i = -1$ mode using $BD3$. Both the two transmitted paths after $BD3$ are modes of $A_i = +1$, while the displaced path after $BD3$ corresponds to $A_i = -1$. After this step, the $A_i = +1$ modes are re-prepared in their eigenstates with $HWP8$, 9, 10, 11 and $BD4$, while the $A_i = -1$ mode is re-created with $HWP15$, $HWP16$ and $BD6$.

In the lower portion of part III, we replace the two originally required two HWPs in this path by $HWP16$ because the polarization state in the transmitted path after $BD6$ is always $|V\rangle$. Thus, HWP16 is used both for eigenstate re-creation and $A_j$ measurement. However, this replacement would not lead to any difference between the two $A_j$ measuring devices, because it can be easily verified that the polarization transformation of two HWPs performed on a definite polarized photon is identical to that of one HWP with a suitable angle setting.

To measure the single observable $\langle A_i\rangle$, the structure of the setup is the same as that for measuring $\langle A_i A_j\rangle$, except that all of the angle settings of the HWPs from $HWP8$ to $HWP18$ are chosen to be 0, $\frac{\pi}{4}$, or $\frac{3\pi}{4}$, so that in the end, single photons are simply directed to certain detectors, without any further interference or measurement.

Part IV contains two polarizing beamsplitters (PBSs), which transmit $|H\rangle$ photons while reflecting $|V\rangle$ photons,

and six fiber-coupled single photon detectors $D_1$ to $D_6$. Interference filters (not shown in Figure 2) with a bandwidth of 3 $nm$ are used before each detector $D_0$ to $D_6$ to remove background photon noise. The coincidence counts $C_{0,n}$ between $D_0$ and $D_n$ $(n = 1, ..., 6)$ are recorded as the experimental results. In experiments measuring $\langle A_i \rangle$, $C_{0,1}$, $C_{0,2}$ and $C_{0,3}$ correspond to $A_i = +1$, and $C_{0,4}$, $C_{0,5}$ and $C_{0,6}$ correspond to $A_i = -1$. However, for the $\langle A_i A_j \rangle$ measuring experiments, $C_{0,1}$ and $C_{0,2}$ correspond to events of $A_i = +1$ and $A_j = +1$; $C_{0,3}$ corresponds to $A_i = +1$ and $A_j = -1$; $C_{0,4}$ and $C_{0,5}$ correspond to $A_i = -1$ and $A_j = +1$; and $C_{0,6}$ corresponds to $A_i = -1$ and $A_j = -1$. Then $\langle A_i A_j \rangle$ is calculated from

$$\begin{aligned} \langle A_i A_j \rangle \ &= \\ P(A_i \ &= \ +1, A_j = +1) - P(A_i = +1, A_j = -1) \\ -P(A_i \ &= \ -1, A_j = +1) + P(A_i = -1, A_j = -1). \end{aligned} \tag{7}$$

Here, $P(A_i = \pm 1, A_j = \pm 1)$ are the joint probabilities of corresponding events, which can be obtained from the measured coincidence counts

$$\begin{aligned} P(A_i \ &= \ +1, A_j = +1) = \frac{C'_{0,1} + C'_{0,2}}{C'_N}, \\ P(A_i \ &= \ +1, A_j = -1) = \frac{C'_{0,3}}{C'_N}, \\ P(A_i \ &= \ -1, A_j = +1) = \frac{C'_{0,4} + C'_{0,5}}{C'_N} \\ P(A_i \ &= \ -1, A_j = -1) = \frac{C'_{0,6}}{C'_N} \end{aligned} \tag{8}$$

where $C'_{0,i}$ is the corresponding coincidence count for $C_{0,i}$ corrected by its relative photon collection efficiency $\eta_i$, and $C'_N = \sum_{i=1}^{6} C'_{0,i}$ is the corrected total coincidence count. To obtain $C'_{0,i}$, we first choose some suitable angle settings for all of the HWPs: the 18 HWPs in the setup are oriented as: 22.5° for HWP15, 45° for HWP5, 13, and 17, 67.5° for HWP7, 9, 14 and 18, while all the other HWPs are oriented in 0°. In such configurations, no interference occurs in the setup, and the relative probabilities $p_i$ of projecting the single photons into the paths before detectors $D1$, $D2$,...,$D6$ are set to be $2 : 1 : 1 : 2 : 1 : 1$. Then, we record the six coincidence counts $C^r_{0,1}$, $C^r_{0,2}$, ... $C^r_{0,6}$ for reference. We let $\eta_6 = 1$, so $\eta_i = \frac{C^r_{0,i}}{p_i C^r_{0,6}}$, and $C'_{0,i} = \frac{C_{0,i}}{\eta_i}$ for $i = 1, 2, ..., 6$.

For each state in Table 1, we measured all 37 expectation values in inequality (5), including the 13 single observables $A_i$ and the 24 compatible observable pairs $A_i A_j$. For example, for the input state $\frac{1}{\sqrt{3}}(|0\rangle + |1\rangle + |2\rangle)$, Table 2 lists the 37 expectation values measured in the experiment versus their QM's predictions. To give out some helpful details of our experiment, we list the measured results for other input states in Table I to Table IV in Appendix A. And the angle settings of all the 18 HWPs in the experiment setup for the 37 measurements of the 8 input states are listed in Table V and Table VI in Appendix B. Table 1 also summarizes the calculated values of $S$ in inequality (5) for the 8 input states; these values are all close to the QM's prediction of $\frac{29}{3}$, and obviously violate the NCHV bound of 9.

This violation demonstrates a state-independent experimental result for a single indivisible three-level system that can not be explained by the NCHV models.

The heralded photon collection efficiency in our experiment is approximately 15%, and we must adopt the fair-sampling assumption, as have all previous experimental tests of hidden variables models performed with photons[7, 22–26].

In our experiment, due to the configuration of the cascaded setup, all of the measurement setups for the same $A_i$ are the same in construction, regardless of the context in which $A_i$ is measured. We only need to take the $A_i$ measuring device as a basic unit and connect it to the two optical paths of the input state. This feature of our setup prevents us from encountering the problem of determining whether setups for the same $A_i$ with different physical structures are the same[11]. Another distinguishing feature of our setup is that it keeps all possible results allowed by NCHV models, even that of $A_i = -1$ and $A_j = -1$, which is impossible in QM. Thus, these features makes our test of NCHV models more basic.

The basic photon interference blocks in the experiment are Mach-Zehnder interferometers (MZIs) composed of two BDs and two HWPs. There are three cascaded MZIs in the upper branch of the whole setup, while only two cascaded MZIs are in the lower branch. For each MZI, we observe an interference fringe with a visibility above 98%. The main advantage of such BD-interferometer is the high phase-stability due to its two parallel and small-separated (center-to-center distance of 4 $mm$) arms. Being placed on a floating optical table, the stable time (with variations smaller than 3%) of its phase difference between two arms is observed to be over 3 hours, which is sufficient for our experiment.

## IV. CONCLUSION

To summarize, our experimental results demonstrate a state-independent contradiction with the predictions of noncontextual realistic theory for an indivisible system. This contradiction precludes NCHV models in the most basic manner. Additionally, this result may add to a deeper understanding of how quantum mechanics differs from classical physics, and this deeper understanding is hoped to inspire wider applications of quantum mechanics.

**Note:** After we submitted this paper, we noticed that a similar work [27] on state-independent experimental test of quantum contextuality in an indivisible system was published on PRL (Phys. Rev. Lett. 109, 150401 (2012)). In their experiment, a scheme of joint measurement on two compatible observables was employed, and the inequality in Ref. [12] was tested.

**Acknowledgement**

We would like to thank SiXia Yu and Choo Hiap Oh for helpful discussions. This work was supported by the National Basic Research Program of China (Grant Nos. 2011CB921200 and 2011CBA00200), the National Natural Science Foundation of China (Grant Nos. 11274289, 11074242, 11104261, 60921091 and 61275122), the National

Science Fund for Distinguished Young Scholars (Grant No. 61225025), the Fundamental Research Funds for the Central Universities (Grant Nos. WK2030020004 and WK2030020007), and the Anhui Provincial Natural Science Foundation (Grant No. 11040606Q47).

[1] A. Einstein, B. Podolsky, and N. Rosen, Phys. Rev. **47**, 777 (1935).
[2] S. Kochen, and E. P. Specker, J. Math. Mech. **17**, 59 (1967).
[3] J. S. Bell, Rev. Mod. Phys. **38**, 447 (1966).
[4] A. Aspect, J. Dalibard, and G. Roger, Phys. Rev. Lett. **49**, 1804 (1982).
[5] G. Weihs, T. Jennewein, C. Simon, H. Weinfurter, and A. Zeilinger, Phys. Rev. Lett. **81**, 5039 (1998).
[6] M. Michler, H. Weinfurter, and M. Żukowski, Phys. Rev. Lett. **84**, 5457–5461 (2000).
[7] Y. -F. Huang, C. -F. Li, Y. -S. Zhang, J. -W. Pan, and G. -C. Guo, Phys. Rev. Lett. **90**, 250401 (2003).
[8] Y. Hasegawa, R. Loidl, G. Badurek, M. Baron, and H. Rauch, Phys. Rev. Lett. **97**, 230401 (2006).
[9] A. Cabello, Phys. Rev. Lett. **101**, 210401 (2008).
[10] G. Kirchmair, F. Zähringer, R. Gerritsma, M. Kleinmann, O. Gühne, A. Cabello, R. Blatt, and C. F. Roos, Nature (London) **460**, 494 (2009).
[11] R. Lapkiewicz, P. Li, C. Schaeff, N. K. Langford, S. Ramelow, M. Wieśniak, and A. Zeilinger, Nature (London) **474**, 490 (2011).
[12] S. -X. Yu, and C. H. Oh, Phys. Rev. Lett. **108**, 030402 (2012).
[13] A. Cabello, A. Elias, B. Kate, B. Mohamed, and B.Ingemar, Phys. Rev. A **85**, 032108 (2012).
[14] N. D. Mermin, Phys. Rev. Lett. **65**, 3373–3376 (1990).
[15] R. Clifton, Am. J. Phys. **61**, 443–447 (1993).
[16] A. Cabello, J. M. Estebaranz, and G. Garcia-Alcaine, Phys. Lett. A **212**, 183–187 (1996).
[17] N. D. Mermin, Rev. Mod Phys, **65**, 803 (1993).
[18] A. Peres, J. Phys. A **24**, L175 (1991).
[19] J. Bub, Found. Phys. **26**, 787 (1996).
[20] J. H. Conway, and S. Kochen, in Quantum [Un]speakables: From Bell to quantum information, edited by R. A. Bertlmann and A. Zeilinger (Springer-Verlag, Berlin, 2002), p. 257.
[21] E. Amselem, M. R$\mathring{a}$dmark, M. Bourennane, and A. Cabello, Phys. Rev. Lett. **103**, 160405 (2009).
[22] A. Aspect, J. Dalibard, G. Roger, Phys. Rev. Lett. **49**, 1804 (1982).
[23] W. Tittel, J. Brendel, H. Zbinden, and N. Gisin, Phys. Rev. Lett. **81**, 3563 (1998).
[24] G. Weihs, T. Jennewein, C. Simon, H. Weinfurter, and A. Zeilinger, Phys. Rev. Lett. **81**, 5039 (1998).
[25] S. Gröblacher, T. Paterek, R. Kaltenbaek, Č. Brukner, M. Żukowski, M. Aspelmeyer, and A. Zeilinger, Nature (London) **446**, 871 (2007).
[26] D. N. Matsukevich, P. Maunz, D. L. Moehring, S. Olmschenk, and C. Monroe, Phys. Rev. Lett. **100**, 150404 (2008).
[27] C. Zu, Y.-X. Wang, D.-L. Deng, X.-Y. Chang, K. Liu, P.-Y. Hou, H.-X. Yang, and L.-M. Duan, Phys. Rev. Lett. **109**, 150401 (2012).

**Figure Legends:**

**Figure 1. Typical single-observable measuring devices.** Experimental setups for measuring $A_3$, $A_7$, $A_{11}$, from top to bottom. $\left|\psi_{A_i}^{+1}\right\rangle$ ($\left|\psi_{A_i}^{-1}\right\rangle$) is the eigenstate of $A_i$ corresponding to the eigenvalue $+1$ ($-1$). BD is the beam displacer. The number accompanying each HWP is the angle of its optical axis relative to the horizontal polarization direction. Red and blue lines show the optical paths for the case of the $\left|\psi_{A_i}^{-1}\right\rangle$ input state. The red line represents the $|V\rangle$ mode in the path while the blue line represents the $|H\rangle$ mode. The red (blue) dotted line indicates that there is no photon in the $|V\rangle$ ($|H\rangle$) mode of this path. The thickness of the line denotes the intensity of the corresponding mode.

**Figure 2. Experimental setup.** Ultraviolet (UV) laser pulses serve as a pump laser for the SPDC process in a BBO crystal. One photon of the twin photons is coupled into a 3-$m$-long polarization-maintaining single-mode fiber (PMF). A GRIN lens (GL) collimates the output beam from the PMF. The polarizer P prepares the photon in the $|H\rangle$ polarization. The dotted blue lines outline the four parts of the experimental setup. Some HWPs (light gray) are always oriented at 0° (or 45°, see Table V and VI in Appendix B for details) and are only used for path length compensation or transformation between $|H\rangle$ and $|V\rangle$. The inset denotes the positions of the four tiltable phase-tuning quarter wave-plates (QWPs), which are inserted in the setup, and are not visible in the main figure. In the experiment, the phase difference of two arms in each MZ interferometer (MZI) is tuned to $2n\pi$ ($n$ being integer) by these tiltable QWPs. $QWP1$ is used for the MZI composed of $BD1$ and $BD2$, $QWP2$ for MZI of $BD2$ and $BD4$, $QWP3$ for MZI of $BD4$ and $BD5$, and $QWP4$ for MZI of $BD6$ and $BD7$. Note that $QWP2$ is inserted after $BD4$ in such a way that both two parallel optical paths after $BD4$ pass through it. Thus when $QWP2$ is tilted, it also changes the phase difference between the $|H\rangle$ mode in the lower path and $|V\rangle$ mode in the upper path besides changing the relative phase between $|H\rangle$ and $|V\rangle$ modes in the upper path. So $QWP3$ after $BD5$ should be tilted only after the tilting angle of $QWP2$ has been fixed.

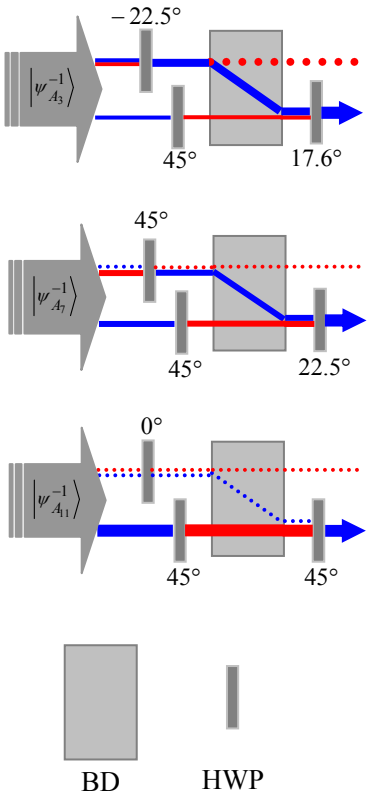
−22.5°
45°
17.6°
45°
45°
22.5°
0°
45°
45°
BD
HWP

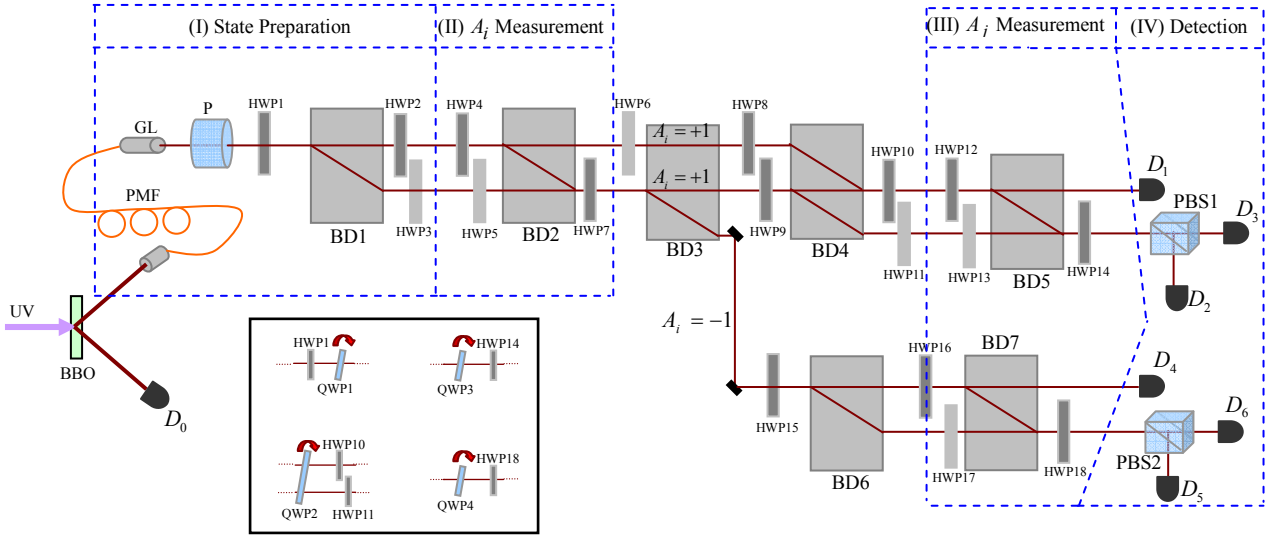
(I) State Preparation
(II) $A_i$ Measurement
(III) $A_i$ Measurement
(IV) Detection
GL
P
HWP1
HWP2
HWP4
HWP6
HWP8
HWP10
HWP12
PMF
BD1
HWP3
HWP5
BD2
HWP7
$A_i = +1$
$A_i = +1$
BD3
HWP9
BD4
HWP11
HWP13
BD5
HWP14
$D_1$
PBS1
$D_3$
$D_2$
UV
BBO
$D_0$
$A_i = -1$
HWP15
BD6
HWP16
BD7
HWP17
HWP18
$D_4$
$D_6$
PBS2
$D_5$
HWP1
QWP1
HWP14
QWP3
HWP10
QWP2
HWP11
HWP18
QWP4

**Table Legends:**

**Table 1:** Experimental results for S´ in inequality (Eq. 5) for eight input qutrit states. The errors in the last line are the corresponding standard deviations calculated according to photon counting statistics. The quantum theoretical prediction of $S'$ for all states is $S' = 9 + \frac{2}{3}$.

**Table 2:** Measured results versus QM's predictions of the 37 observables for the particular input qutrit state $\frac{1}{\sqrt{3}}(|0\rangle + |1\rangle + |2\rangle)$. All of the errors are calculated from photon counting statistics.

## Appendix A: Measured results of the other 7 input states

| **Input state** $\|0\rangle$ | | | | | | | | |
|---|---|---|---|---|---|---|---|---|
| Terms | Measured results | Theoretical values | Terms | Measured results | Theoretical values | Terms | Measured results | Theoretical values |
| $\langle A_1 \rangle$ | 0.3173±0.0026 | 0.3333 | $\langle A_1 A_6 \rangle$ | 0.3300±0.0027 | 0.3333 | $\langle A_5 A_{11} \rangle$ | -0.9937±0.0003 | -1 |
| $\langle A_2 \rangle$ | 0.2929±0.0026 | 0.3333 | $\langle A_1 A_7 \rangle$ | -0.6508±0.0022 | -0.6667 | $\langle A_6 A_{11} \rangle$ | -0.9913±0.0004 | -1 |
| $\langle A_3 \rangle$ | 0.2931±0.0026 | 0.3333 | $\langle A_1 A_9 \rangle$ | -0.6899±0.0021 | -0.6667 | $\langle A_5 A_6 \rangle$ | 0.9922±0.0003 | 1 |
| $\langle A_4 \rangle$ | 0.3035±0.0026 | 0.3333 | $\langle A_2 A_5 \rangle$ | 0.3096±0.0027 | 0.3333 | $\langle A_7 A_{12} \rangle$ | -0.0316±0.0028 | 0 |
| $\langle A_5 \rangle$ | 0.9949±0.0003 | 1 | $\langle A_2 A_8 \rangle$ | -0.6743±0.0022 | -0.6667 | $\langle A_8 A_{12} \rangle$ | -0.0375±0.0028 | 0 |
| $\langle A_6 \rangle$ | 0.9953±0.0003 | 1 | $\langle A_2 A_9 \rangle$ | -0.6918±0.0021 | -0.6667 | $\langle A_7 A_8 \rangle$ | -0.9805±0.0006 | -1 |
| $\langle A_7 \rangle$ | -0.0439±0.0028 | 0 | $\langle A_3 A_5 \rangle$ | 0.3078±0.0027 | 0.3333 | $\langle A_9 A_{13} \rangle$ | -0.0361±0.0029 | 0 |
| $\langle A_8 \rangle$ | -0.0427±0.0028 | 0 | $\langle A_3 A_7 \rangle$ | -0.6595±0.0022 | -0.6667 | $\langle A_{10} A_{13} \rangle$ | -0.0186±0.0028 | 0 |
| $\langle A_9 \rangle$ | -0.0442±0.0028 | 0 | $\langle A_3 A_{10} \rangle$ | -0.6967±0.0021 | -0.6667 | $\langle A_9 A_{10} \rangle$ | -0.9781±0.0006 | -1 |
| $\langle A_{10} \rangle$ | -0.0387±0.0028 | 0 | $\langle A_4 A_6 \rangle$ | 0.3101±0.0027 | 0.3333 | $\langle A_{11} A_{12} \rangle$ | -0.9911±0.0004 | -1 |
| $\langle A_{11} \rangle$ | -0.9946±0.0003 | -1 | $\langle A_4 A_8 \rangle$ | -0.6496±0.0022 | -0.6667 | $\langle A_{12} A_{13} \rangle$ | 0.9941±0.0003 | 1 |
| $\langle A_{12} \rangle$ | 0.9954±0.0003 | 1 | $\langle A_4 A_{10} \rangle$ | -0.6752±0.0022 | -0.6667 | $\langle A_{11} A_{13} \rangle$ | -0.9928±0.0004 | -1 |
| $\langle A_{13} \rangle$ | 0.9946±0.0003 | 1 | | | | | | |

| **Input state** $\|1\rangle$ | | | | | | | | |
|---|---|---|---|---|---|---|---|---|
| Terms | Measured results | Theoretical values | Terms | Measured results | Theoretical values | Terms | Measured results | Theoretical values |
| $\langle A_1 \rangle$ | 0.3161±0.0023 | 0.3333 | $\langle A_1 A_6 \rangle$ | -0.6923±0.0018 | -0.6667 | $\langle A_5 A_{11} \rangle$ | 0.0077±0.0024 | 0 |
| $\langle A_2 \rangle$ | 0.3094±0.0023 | 0.3333 | $\langle A_1 A_7 \rangle$ | 0.3186±0.0024 | 0.3333 | $\langle A_6 A_{11} \rangle$ | -0.0351±0.0024 | 0 |
| $\langle A_3 \rangle$ | 0.3020±0.0023 | 0.3333 | $\langle A_1 A_9 \rangle$ | -0.6469±0.0020 | -0.6667 | $\langle A_5 A_6 \rangle$ | -0.9885±0.0004 | -1 |
| $\langle A_4 \rangle$ | 0.2602±0.0023 | 0.3333 | $\langle A_2 A_5 \rangle$ | -0.6866±0.0019 | -0.6667 | $\langle A_7 A_{12} \rangle$ | -0.9875±0.0005 | -1 |
| $\langle A_5 \rangle$ | 0.0011±0.0024 | 0 | $\langle A_2 A_8 \rangle$ | 0.2644±0.0025 | 0.3333 | $\langle A_8 A_{12} \rangle$ | -0.9839±0.0006 | -1 |
| $\langle A_6 \rangle$ | -0.0263±0.0024 | 0 | $\langle A_2 A_9 \rangle$ | -0.6636±0.0021 | -0.6667 | $\langle A_7 A_8 \rangle$ | 0.9902±0.0004 | 1 |
| $\langle A_7 \rangle$ | 0.9926±0.0003 | 1 | $\langle A_3 A_5 \rangle$ | -0.6535±0.0021 | -0.6667 | $\langle A_9 A_{13} \rangle$ | -0.0127±0.0024 | 0 |
| $\langle A_8 \rangle$ | 0.9968±0.0002 | 1 | $\langle A_3 A_7 \rangle$ | 0.2798±0.0026 | 0.3333 | $\langle A_{10} A_{13} \rangle$ | -0.0062±0.0028 | 0 |
| $\langle A_9 \rangle$ | -0.0383±0.0025 | 0 | $\langle A_3 A_{10} \rangle$ | -0.6979±0.0020 | -0.6667 | $\langle A_9 A_{10} \rangle$ | -0.9794±0.0006 | -1 |
| $\langle A_{10} \rangle$ | 0.0227±0.0025 | 0 | $\langle A_4 A_6 \rangle$ | -0.7034±0.0020 | -0.6667 | $\langle A_{11} A_{12} \rangle$ | -0.9856±0.0006 | -1 |
| $\langle A_{11} \rangle$ | 0.9925±0.0003 | 1 | $\langle A_4 A_8 \rangle$ | 0.2665±0.0026 | 0.3333 | $\langle A_{12} A_{13} \rangle$ | -0.9923±0.0003 | -1 |
| $\langle A_{12} \rangle$ | -0.9906±0.0003 | -1 | $\langle A_4 A_{10} \rangle$ | -0.6100±0.0023 | -0.6667 | $\langle A_{11} A_{13} \rangle$ | 0.9912±0.0003 | 1 |
| $\langle A_{13} \rangle$ | 0.9967±0.0002 | 1 | | | | | | |

TABLE I: Measured results of the 37 terms in the KS inequality (5) for input states of $|0\rangle$ and $|1\rangle$.

| **Input state** $\|2\rangle$ | | | | | | | | |
|---|---|---|---|---|---|---|---|---|
| Terms | Measured results | Theoretical values | Terms | Measured results | Theoretical values | Terms | Measured results | Theoretical values |
| $\langle A_1 \rangle$ | 0.3442±0.0023 | 0.3333 | $\langle A_1 A_6 \rangle$ | -0.6228±0.0019 | -0.6667 | $\langle A_5 A_{11} \rangle$ | -0.0168±0.0025 | 0 |
| $\langle A_2 \rangle$ | 0.3450±0.0023 | 0.3333 | $\langle A_1 A_7 \rangle$ | -0.6694±0.0018 | -0.6667 | $\langle A_6 A_{11} \rangle$ | 0.0236±0.0004 | 0 |
| $\langle A_3 \rangle$ | 0.2908±0.0023 | 0.3333 | $\langle A_1 A_9 \rangle$ | 0.3370±0.0023 | 0.3333 | $\langle A_5 A_6 \rangle$ | -0.9880±0.0025 | -1 |
| $\langle A_4 \rangle$ | 0.3357±0.0023 | 0.3333 | $\langle A_2 A_5 \rangle$ | -0.6553±0.0019 | -0.6667 | $\langle A_7 A_{12} \rangle$ | -0.0168±0.0025 | 0 |
| $\langle A_5 \rangle$ | 0.0105±0.0024 | 0 | $\langle A_2 A_8 \rangle$ | -0.6099±0.0020 | -0.6667 | $\langle A_8 A_{12} \rangle$ | 0.0135±0.0005 | 0 |
| $\langle A_6 \rangle$ | 0.0191±0.0024 | 0 | $\langle A_2 A_9 \rangle$ | 0.3428±0.0023 | 0.3333 | $\langle A_7 A_8 \rangle$ | -0.9778±0.0003 | -1 |
| $\langle A_7 \rangle$ | -0.0112±0.0025 | 0 | $\langle A_3 A_5 \rangle$ | -0.7535±0.0016 | -0.6667 | $\langle A_9 A_{13} \rangle$ | -0.9936±0.0004 | -1 |
| $\langle A_8 \rangle$ | 0.0437±0.0025 | 0 | $\langle A_3 A_7 \rangle$ | -0.5557±0.0021 | -0.6667 | $\langle A_{10} A_{13} \rangle$ | -0.9869±0.0003 | -1 |
| $\langle A_9 \rangle$ | 0.9961±0.0002 | 1 | $\langle A_3 A_{10} \rangle$ | 0.2665±0.0024 | 0.3333 | $\langle A_9 A_{10} \rangle$ | 0.9946±0.0003 | 1 |
| $\langle A_{10} \rangle$ | 0.9961±0.0002 | 1 | $\langle A_4 A_6 \rangle$ | -0.6320±0.0019 | -0.6667 | $\langle A_{11} A_{12} \rangle$ | 0.9927±0.0004 | 1 |
| $\langle A_{11} \rangle$ | 0.9936±0.0003 | 1 | $\langle A_4 A_8 \rangle$ | -0.6757±0.0018 | -0.6667 | $\langle A_{12} A_{13} \rangle$ | -0.9901±0.0003 | -1 |
| $\langle A_{12} \rangle$ | 0.9985±0.0001 | 1 | $\langle A_4 A_{10} \rangle$ | 0.3362±0.0023 | 0.3333 | $\langle A_{11} A_{13} \rangle$ | -0.9922±0.0024 | -1 |
| $\langle A_{13} \rangle$ | -0.9936±0.0003 | -1 | | | | | | |

| **Input state** $(\|0\rangle+\|1\rangle)/\sqrt{2}$ | | | | | | | | |
|---|---|---|---|---|---|---|---|---|
| Terms | Measured results | Theoretical values | Terms | Measured results | Theoretical values | Terms | Measured results | Theoretical values |
| $\langle A_1 \rangle$ | 0.9886±0.0004 | 1 | $\langle A_1 A_6 \rangle$ | 0.4709±0.0022 | 0.5 | $\langle A_5 A_{11} \rangle$ | -0.4251±0.0022 | -0.5 |
| $\langle A_2 \rangle$ | 0.9881±0.0004 | 1 | $\langle A_1 A_7 \rangle$ | 0.5361±0.0021 | 0.5 | $\langle A_6 A_{11} \rangle$ | -0.4587±0.0021 | -0.5 |
| $\langle A_3 \rangle$ | -0.3191±0.0023 | -0.3333 | $\langle A_1 A_9 \rangle$ | -0.9638±0.0007 | -1 | $\langle A_5 A_6 \rangle$ | -0.0114±0.0024 | 0 |
| $\langle A_4 \rangle$ | -0.3165±0.0023 | -0.3333 | $\langle A_2 A_5 \rangle$ | 0.4861±0.0021 | 0.5 | $\langle A_7 A_{12} \rangle$ | -0.5130±0.0021 | -0.5 |
| $\langle A_5 \rangle$ | 0.4896±0.0022 | 0.5 | $\langle A_2 A_8 \rangle$ | 0.4804±0.0021 | 0.5 | $\langle A_8 A_{12} \rangle$ | -0.5419±0.0021 | -0.5 |
| $\langle A_6 \rangle$ | 0.4729±0.0022 | 0.5 | $\langle A_2 A_9 \rangle$ | -0.9767±0.0005 | -1 | $\langle A_7 A_8 \rangle$ | 0.0267±0.0025 | 0 |
| $\langle A_7 \rangle$ | 0.5420±0.0021 | 0.5 | $\langle A_3 A_5 \rangle$ | -0.8384±0.0013 | -0.8333 | $\langle A_9 A_{13} \rangle$ | -0.9780±0.0005 | -1 |
| $\langle A_8 \rangle$ | 0.5225±0.0021 | 0.5 | $\langle A_3 A_7 \rangle$ | -0.7712±0.0016 | -0.8333 | $\langle A_{10} A_{13} \rangle$ | 0.9851±0.0004 | 1 |
| $\langle A_9 \rangle$ | -0.9787±0.0005 | -1 | $\langle A_3 A_{10} \rangle$ | -0.3344±0.0023 | -0.3333 | $\langle A_9 A_{10} \rangle$ | -0.9724±0.0006 | -1 |
| $\langle A_{10} \rangle$ | 0.9864±0.0004 | 1 | $\langle A_4 A_6 \rangle$ | -0.8423±0.0013 | -0.8333 | $\langle A_{11} A_{12} \rangle$ | -0.9931±0.0003 | -1 |
| $\langle A_{11} \rangle$ | 0.1070±0.0025 | 0 | $\langle A_4 A_8 \rangle$ | -0.8001±0.0015 | -0.8333 | $\langle A_{12} A_{13} \rangle$ | -0.0013±0.0024 | 0 |
| $\langle A_{12} \rangle$ | -0.0067±0.0025 | 0 | $\langle A_4 A_{10} \rangle$ | -0.3205±0.0023 | -0.3333 | $\langle A_{11} A_{13} \rangle$ | 0.0554±0.0024 | 0 |
| $\langle A_{13} \rangle$ | 0.9973±0.0002 | 1 | | | | | | |

TABLE II: Measured results of the 37 terms in the inequality (5) for input states of $|2\rangle$ and $\frac{1}{\sqrt{2}}(|0\rangle+|1\rangle)$.

| **Input state** $(\|0\rangle+\|2\rangle)/\sqrt{2}$ | | | | | | | | |
|---|---|---|---|---|---|---|---|---|
| Terms | Measured results | Theoretical values | Terms | Measured results | Theoretical values | Terms | Measured results | Theoretical values |
| $\langle A_1 \rangle$ | 0.9866±0.0003 | 1 | $\langle A_1 A_6 \rangle$ | 0.4796±0.0023 | 0.5 | $\langle A_5 A_{11} \rangle$ | -0.4263±0.0023 | -0.5 |
| $\langle A_2 \rangle$ | -0.2886±0.0020 | -0.3333 | $\langle A_1 A_7 \rangle$ | -0.9658±0.0007 | -1 | $\langle A_6 A_{11} \rangle$ | -0.4796±0.0022 | -0.5 |
| $\langle A_3 \rangle$ | 0.9871±0.0003 | 1 | $\langle A_1 A_9 \rangle$ | 0.4640±0.0022 | 0.5 | $\langle A_5 A_6 \rangle$ | 0.0481±0.0025 | 0 |
| $\langle A_4 \rangle$ | -0.3143±0.0019 | -0.3333 | $\langle A_2 A_5 \rangle$ | -0.8301±0.0013 | -0.8333 | $\langle A_7 A_{12} \rangle$ | -0.9798±0.0005 | -1 |
| $\langle A_5 \rangle$ | 0.5319±0.0018 | 0.5 | $\langle A_2 A_8 \rangle$ | -0.3003±0.0023 | -0.3333 | $\langle A_8 A_{12} \rangle$ | 0.9861±0.0004 | 1 |
| $\langle A_6 \rangle$ | 0.4965±0.0018 | 0.5 | $\langle A_2 A_9 \rangle$ | -0.7782±0.0015 | -0.8333 | $\langle A_7 A_8 \rangle$ | -0.9721±0.0006 | -1 |
| $\langle A_7 \rangle$ | -0.9760±0.0004 | -1 | $\langle A_3 A_5 \rangle$ | 0.4566±0.0021 | 0.5 | $\langle A_9 A_{13} \rangle$ | -0.5023±0.0021 | -0.5 |
| $\langle A_8 \rangle$ | 0.9849±0.0004 | 1 | $\langle A_3 A_7 \rangle$ | -0.9469±0.0008 | -1 | $\langle A_{10} A_{13} \rangle$ | -0.4973±0.0021 | -0.5 |
| $\langle A_9 \rangle$ | 0.5454±0.0017 | 0.5 | $\langle A_3 A_{10} \rangle$ | 0.5820±0.0019 | 0.5 | $\langle A_9 A_{10} \rangle$ | -0.0268±0.0025 | 0 |
| $\langle A_{10} \rangle$ | 0.5514±0.0017 | 0.5 | $\langle A_4 A_6 \rangle$ | -0.8257±0.0013 | -0.8333 | $\langle A_{11} A_{12} \rangle$ | -0.0145±0.0024 | 0 |
| $\langle A_{11} \rangle$ | 0.0929±0.0021 | 0 | $\langle A_4 A_8 \rangle$ | -0.3100±0.0023 | -0.3333 | $\langle A_{12} A_{13} \rangle$ | 0.0130±0.0024 | 0 |
| $\langle A_{12} \rangle$ | 0.9974±0.0002 | 1 | $\langle A_4 A_{10} \rangle$ | -0.7701±0.0016 | -0.8333 | $\langle A_{11} A_{13} \rangle$ | -0.9953±0.0002 | -1 |
| $\langle A_{13} \rangle$ | -0.0418±0.0020 | 0 | | | | | | |

| **Input state** $(\|1\rangle+\|2\rangle)/\sqrt{2}$ | | | | | | | | |
|---|---|---|---|---|---|---|---|---|
| Terms | Measured results | Theoretical values | Terms | Measured results | Theoretical values | Terms | Measured results | Theoretical values |
| $\langle A_1 \rangle$ | -0.3730±0.0024 | -0.3333 | $\langle A_1 A_6 \rangle$ | -0.3632±0.0025 | -0.3333 | $\langle A_5 A_{11} \rangle$ | -0.9967±0.0002 | -1 |
| $\langle A_2 \rangle$ | 0.9957±0.0003 | 1 | $\langle A_1 A_7 \rangle$ | -0.8234±0.0017 | -0.8333 | $\langle A_6 A_{11} \rangle$ | 0.9926±0.0003 | 1 |
| $\langle A_3 \rangle$ | 0.9972±0.0002 | 1 | $\langle A_1 A_9 \rangle$ | -0.8319±0.0017 | -0.8333 | $\langle A_5 A_6 \rangle$ | -0.9963±0.0002 | -1 |
| $\langle A_4 \rangle$ | -0.3448±0.0025 | -0.3333 | $\langle A_2 A_5 \rangle$ | -0.9941±0.0003 | -1 | $\langle A_7 A_{12} \rangle$ | -0.4934±0.0024 | -0.5 |
| $\langle A_5 \rangle$ | -0.9963±0.0002 | -1 | $\langle A_2 A_8 \rangle$ | 0.4012±0.0027 | 0.5 | $\langle A_8 A_{12} \rangle$ | -0.5518±0.0023 | -0.5 |
| $\langle A_6 \rangle$ | 0.9977±0.0002 | 1 | $\langle A_2 A_9 \rangle$ | 0.5167±0.0025 | 0.5 | $\langle A_7 A_8 \rangle$ | 0.0288±0.0027 | 0 |
| $\langle A_7 \rangle$ | 0.5185±0.0023 | 0.5 | $\langle A_3 A_5 \rangle$ | -0.9927±0.0004 | -1 | $\langle A_9 A_{13} \rangle$ | -0.3753±0.0026 | -0.5 |
| $\langle A_8 \rangle$ | 0.4744±0.0024 | 0.5 | $\langle A_3 A_7 \rangle$ | 0.4721±0.0025 | 0.5 | $\langle A_{10} A_{13} \rangle$ | -0.4814±0.0024 | -0.5 |
| $\langle A_9 \rangle$ | 0.4989±0.0024 | 0.5 | $\langle A_3 A_{10} \rangle$ | 0.4636±0.0024 | 0.5 | $\langle A_9 A_{10} \rangle$ | -0.0305±0.0028 | 0 |
| $\langle A_{10} \rangle$ | 0.4587±0.0024 | 0.5 | $\langle A_4 A_6 \rangle$ | -0.3152±0.0026 | -0.3333 | $\langle A_{11} A_{12} \rangle$ | -0.1265±0.0027 | 0 |
| $\langle A_{11} \rangle$ | 0.9955±0.0003 | 1 | $\langle A_4 A_8 \rangle$ | -0.8103±0.0017 | -0.8333 | $\langle A_{12} A_{13} \rangle$ | -0.9951±0.0003 | -1 |
| $\langle A_{12} \rangle$ | -0.0411±0.0027 | 0 | $\langle A_4 A_{10} \rangle$ | -0.8001±0.0018 | -0.8333 | $\langle A_{11} A_{13} \rangle$ | 0.0527±0.0027 | 0 |
| $\langle A_{13} \rangle$ | -0.0040±0.0027 | 0 | | | | | | |

TABLE III: Measured results of the 37 terms in the inequality (5) for input states of $\frac{1}{\sqrt{2}}(|0\rangle+|2\rangle)$ and $\frac{1}{\sqrt{2}}(|1\rangle+|2\rangle)$.

| **Input state** $\rho_I = (\|0\rangle\langle 0\| + \|1\rangle\langle 1\| + \|2\rangle\langle 2\|)/3$ | | | | | | | | |
|---|---|---|---|---|---|---|---|---|
| Terms | Measured results | Theoretical values | Terms | Measured results | Theoretical values | Terms | Measured results | Theoretical values |
| $\langle A_1 \rangle$ | 0.3218±0.0027 | 0.3333 | $\langle A_1 A_6 \rangle$ | -0.3064±0.0024 | -0.3333 | $\langle A_5 A_{11} \rangle$ | -0.4107±0.0023 | -0.3333 |
| $\langle A_2 \rangle$ | 0.3604±0.0027 | 0.3333 | $\langle A_1 A_7 \rangle$ | -0.3807±0.0025 | -0.3333 | $\langle A_6 A_{11} \rangle$ | -0.3072±0.0024 | -0.3333 |
| $\langle A_3 \rangle$ | 0.3713±0.0026 | 0.3333 | $\langle A_1 A_9 \rangle$ | -0.3562±0.0025 | -0.3333 | $\langle A_5 A_6 \rangle$ | -0.2575±0.0025 | -0.3333 |
| $\langle A_4 \rangle$ | 0.3145±0.0027 | 0.3333 | $\langle A_2 A_5 \rangle$ | -0.3568±0.0026 | -0.3333 | $\langle A_7 A_{12} \rangle$ | -0.3052±0.0025 | -0.3333 |
| $\langle A_5 \rangle$ | 0.3310±0.0027 | 0.3333 | $\langle A_2 A_8 \rangle$ | -0.3001±0.0027 | -0.3333 | $\langle A_8 A_{12} \rangle$ | -0.3028±0.0025 | -0.3333 |
| $\langle A_6 \rangle$ | 0.4117±0.0026 | 0.3333 | $\langle A_2 A_9 \rangle$ | -0.2884±0.0027 | -0.3333 | $\langle A_7 A_8 \rangle$ | -0.3412±0.0026 | -0.3333 |
| $\langle A_7 \rangle$ | 0.3151±0.0027 | 0.3333 | $\langle A_3 A_5 \rangle$ | -0.3196±0.0026 | -0.3333 | $\langle A_9 A_{13} \rangle$ | -0.3341±0.0025 | -0.3333 |
| $\langle A_8 \rangle$ | 0.3186±0.0027 | 0.3333 | $\langle A_3 A_7 \rangle$ | -0.2901±0.0027 | -0.3333 | $\langle A_{10} A_{13} \rangle$ | -0.3625±0.0025 | -0.3333 |
| $\langle A_9 \rangle$ | 0.3384±0.0026 | 0.3333 | $\langle A_3 A_{10} \rangle$ | -0.2501±0.0027 | -0.3333 | $\langle A_9 A_{10} \rangle$ | -0.2707±0.0028 | -0.3333 |
| $\langle A_{10} \rangle$ | 0.3355±0.0028 | 0.3333 | $\langle A_4 A_6 \rangle$ | -0.2905±0.0024 | -0.3333 | $\langle A_{11} A_{12} \rangle$ | -0.3125±0.0026 | -0.3333 |
| $\langle A_{11} \rangle$ | 0.2753±0.0027 | 0.3333 | $\langle A_4 A_8 \rangle$ | -0.3679±0.0025 | -0.3333 | $\langle A_{12} A_{13} \rangle$ | -0.3425±0.0025 | -0.3333 |
| $\langle A_{12} \rangle$ | 0.3981±0.0027 | 0.3333 | $\langle A_4 A_{10} \rangle$ | -0.3317±0.0026 | -0.3333 | $\langle A_{11} A_{13} \rangle$ | -0.3501±0.0026 | -0.3333 |
| $\langle A_{13} \rangle$ | 0.3462±0.0027 | 0.3333 | | | | | | |

TABLE IV: Measured results of the 37 terms in the inequality (5) for the input state being maximally mixed state $\rho_I = (\|0\rangle\langle 0\| + \|1\rangle\langle 1\| + \|2\rangle\langle 2\|)/3$.

### Appendix B: Angle settings of all HWPs

| Input state | $\|0\rangle$ | $\|1\rangle$ | $\|2\rangle$ | $\frac{1}{\sqrt{2}}(\|0\rangle + \|1\rangle)$ | $\frac{1}{\sqrt{2}}(\|0\rangle + \|2\rangle)$ | $\frac{1}{\sqrt{2}}(\|1\rangle + \|2\rangle)$ | $\frac{1}{\sqrt{3}}(\|0\rangle + \|1\rangle + \|2\rangle)$ | $\rho_I$ |
|---|---|---|---|---|---|---|---|---|
| $\theta_1$ | 0° | 45° | 45° | 22.5° | 22.5° | 45° | 27.4° | 27.4° |
| $\theta_2$ | 0° | 45° | 0° | 45° | 0° | 67.5° | 67.5° | 67.5° |
| $\theta_3$ | 0° | 0° | 0° | 0° | 0° | 0° | 0° | 0° |

TABLE V: Angle settings of HWP1, 2 and 3 for the eight input states. And $\theta_i$ stands for HWPi.

| Observable | $\theta_4$ | $\theta_7$ | $\theta_8$ | $\theta_9$ | $\theta_{10}$ | $\theta_{12}$ | $\theta_{14}$ | $\theta_{15}$ | $\theta_{16}$ | $\theta_{18}$ |
|---|---|---|---|---|---|---|---|---|---|---|
| $\langle A_1 \rangle$ | 22.5° | -17.6° | 45° | 135° | 45° | 0° | 0° | 45° | 45° | 45° |
| $\langle A_2 \rangle$ | 67.5° | 17.6° | 45° | 135° | 45° | 0° | 0° | 45° | 45° | 45° |
| $\langle A_3 \rangle$ | -22.5° | 17.6° | 45° | 135° | 45° | 0° | 0° | 45° | 45° | 45° |
| $\langle A_4 \rangle$ | 22.5° | 17.6° | 45° | 135° | 45° | 0° | 0° | 45° | 45° | 45° |
| $\langle A_5 \rangle$ | 22.5° | 0° | 45° | 135° | 45° | 0° | 0° | 45° | 45° | 45° |
| $\langle A_6 \rangle$ | -22.5° | 0° | 45° | 135° | 45° | 0° | 0° | 45° | 45° | 45° |
| $\langle A_7 \rangle$ | 45° | 22. 5° | 45° | 135° | 45° | 0° | 0° | 45° | 45° | 45° |
| $\langle A_8 \rangle$ | 45° | -22.5° | 45° | 135° | 45° | 0° | 0° | 45° | 45° | 45° |
| $\langle A_9 \rangle$ | 0° | 22.5° | 45° | 135° | 45° | 0° | 0° | 45° | 45° | 45° |
| $\langle A_{10} \rangle$ | 0° | -22.5° | 45° | 135° | 45° | 0° | 0° | 45° | 45° | 45° |
| $\langle A_{11} \rangle$ | 0° | 45° | 45° | 135° | 45° | 0° | 0° | 45° | 45° | 45° |
| $\langle A_{12} \rangle$ | 0° | 0° | 45° | 135° | 45° | 0° | 0° | 45° | 45° | 45° |
| $\langle A_{13} \rangle$ | 45° | 0° | 45° | 135° | 45° | 0° | 0° | 45° | 45° | 45° |
| $\langle A_1 A_6 \rangle$ | 22.5° | -17.6° | 45° | 152.6° | 67.5° | -22.5° | 0° | 62.6° | 0° | 0° |
| $\langle A_1 A_7 \rangle$ | 22.5° | -17.6° | 45° | 152.6° | 67.5° | 45° | 22.5° | 62.6° | 67.5° | 22.5° |
| $\langle A_1 A_9 \rangle$ | 22.5° | -17.6° | 45° | 152.6° | 67.5° | 0° | 22.5° | 62.6° | 22.5° | 22.5° |
| $\langle A_2 A_5 \rangle$ | 67.5° | 17.6° | -45° | 152.6° | 22.5° | 22.5° | 0° | -27.4° | 90° | 0° |
| $\langle A_2 A_8 \rangle$ | 67.5° | 17.6° | -45° | 152.6° | 22.5° | 45° | -22.5° | -27.4° | 22.5° | 22.5° |
| $\langle A_2 A_9 \rangle$ | 67.5° | 17.6° | -45° | 152.6° | 22.5° | 0° | 22.5° | -27.4° | 67.5° | 22.5° |
| $\langle A_3 A_5 \rangle$ | -22.5° | 17.6° | 45° | 117.4° | 22.5° | 22.5° | 0° | 27.4° | 90° | 0° |
| $\langle A_3 A_7 \rangle$ | -22.5° | 17.6° | 45° | 117.4° | 22.5° | 45° | 22.5° | 27.4° | 22.5° | -22.5° |
| $\langle A_3 A_{10} \rangle$ | -22.5° | 17.6° | 45° | 117.4° | 22.5° | 0° | -22.5° | 27.4° | 67.5° | -22.5° |
| $\langle A_4 A_6 \rangle$ | 22.5° | 17.6° | -45° | 152.6° | -22.5° | -22.5° | 0° | 27.4° | 0° | 0° |
| $\langle A_4 A_8 \rangle$ | 22.5° | 17.6° | -45° | 152.6° | -22.5° | 45° | -22.5° | 27.4° | 67.5° | -22.5° |
| $\langle A_4 A_{10} \rangle$ | 22.5° | 17.6° | -45° | 152.6° | -22.5° | 0° | -22.5° | 27.4° | 22.5° | -22.5° |
| $\langle A_5 A_{11} \rangle$ | 22.5° | 0° | 45° | 135° | 67.5° | -22.5° | 45° | 45° | 90° | 45° |
| $\langle A_6 A_{11} \rangle$ | -22.5° | 0° | 45° | 135° | 22.5° | 22.5° | 45° | 45° | 90° | 45° |
| $\langle A_5 A_6 \rangle$ | 22.5° | 0° | 45° | 135° | 67.5° | -22.5° | 0° | 45° | 0° | 0° |
| $\langle A_7 A_{12} \rangle$ | 45° | 22. 5° | -45° | 157.5° | 0° | 0° | 0° | -22.5° | 90° | 0° |
| $\langle A_8 A_{12} \rangle$ | 45° | -22.5° | -45° | 112.5° | 0° | 0° | 0° | 22.5° | 90° | 0° |
| $\langle A_7 A_8 \rangle$ | 45° | 22.5° | -45° | 157.5° | 0° | 45° | -22.5° | -22.5° | 45° | 22.5° |
| $\langle A_9 A_{13} \rangle$ | 0° | 22.5° | 45° | 112.5° | 45° | 45° | 0° | 22.5° | 90° | 0° |
| $\langle A_{10} A_{13} \rangle$ | 0° | -22.5° | 45° | 157.5° | 45° | 45° | 0° | -22.5° | 90° | 0° |
| $\langle A_9 A_{10} \rangle$ | 0° | 22.5° | 45° | 112.5° | 45° | 0° | -22.5° | 22.5° | 45° | -22.5° |
| $\langle A_{11} A_{12} \rangle$ | 0° | 45° | 45° | 90° | 45° | 0° | 0° | 0° | 90° | 0° |
| $\langle A_{12} A_{13} \rangle$ | 0° | 0° | 45° | 135° | 45° | 45° | 0° | 45° | 90° | 0° |
| $\langle A_{11} A_{13} \rangle$ | 0° | 45° | 45° | 90° | 45° | 45° | 0° | 0° | 45° | 0° |

TABLE VI: Angle settings of all the other 15 HWPs. Some HWPs are always oriented in the same angle for every measurements and are not listed in the table. These HWPs are: HWP5 (45°), HWP6 (0°), HWP11 (0°), HWP13 (45°), HWP17 (45°).